35th Annual International Conference of the IEEE EMBS
Osaka, Japan, 3 - 7 July, 2013

# Wavelet Based Sparse Source Imaging Technique

Lei Ding, *Member, IEEE*, Min Zhu, *Student Member, IEEE*, Ke Liao

***Abstract*—The present study proposed a novel multi-resolution wavelet to efficiently compress cortical current densities on the highly convoluted cortical surface. The basis function of the proposed wavelet is supported on triangular faces of the cortical mesh and it is thus named as the face-based wavelet to be distinguished from other vertex-based wavelets. The proposed face-based wavelet was used as a transform to gain the sparse representation of cortical sources and then was integrated into the framework of L1-norm regularizations with the purpose to improve the performance of sparse source imaging (SSI) in solving EEG/MEG inverse problems. Monte Carlo simulations were conducted with multiple extended sources (up to ten) at random locations. Experimental MEG data from an auditory induced language task was further adopted to evaluate the performance of the proposed wavelet based SSI technique. The present results indicated that the face-based wavelet can efficiently compress cortical current densities and has better performance than the vertex-based wavelet in helping inverse source reconstructions in terms of estimation accuracies in source localization and source extent. Experimental results further indicated improved detection performance of the face-based wavelet as compared with the vertex-based wavelet in the framework of SSI. It thus suggests the proposed wavelet based SSI can become a promising tool in studying brain functions and networks.**

## I. Introduction

The cerebral cortex of the human is a thin sheet of gray matters, where believed lays dominant generators for electroencephalography (EEG) and magnetoencephalography (MEG) signals [1]. Cortical current density (CCD) model [2] has been widely adopted to model the source space for EEG/MEG inverse problems with thousands or ten thousands of continuously distributed dipoles on the cortical surface. However, the number of EEG/MEG measurements is limited to a few hundreds, making EEG/MEG inverse problems highly underdetermined. Regularizations are commonly used strategies to search for a unique solution by placing priors [3].

Regularizations using L1 norm [4-7] recently attract more attentions due to its sparse solutions that only small fractions of the brain are active, which is the case in most experimental EEG/MEG studies [8]. However, the direct use of L1 norm in original source domain in classic L1-norm regularization methods [5] usually resulted in over-focus reconstructions with highly underestimated source extents [6], while it is critical in many clinical applications to accurately estimate source extents, e.g. identification of epileptic tissues and eloquent function areas for brain resections in epilepsy patients [9]. According to the information theory, sparse solutions can also be achieved in a transformed domain where cortical current densities can be sparser or more compressible [10]. Seeking suitable transforms to sparsely represent cortical current densities is thus of importance. A new sparse source imaging (SSI) technique exploring the sparseness in the variation domain has been developed and proved to be able to address the over-focus problem [6].

It is well known that wavelet is a powerful tool for compressing signals [11]. Wavelet coefficients for natural signals are mostly zero or negligibly small, which makes signals sparse or compressible in the wavelet domain. The fact makes the wavelet transform a useful representation of cortical current densities in L1-norm regularization methods for solving EEG/MEG inverse problems. However, since the structure of cortical surface is highly convoluted and irregular, wavelets defined on regular shaped spaces cannot be used. Modified wavelets have been developed on arbitrary spaces in computer graphic and geometry compression, e.g. Spherical wavelets [12], irregular wavelets [13], and blending of linear and constant (BLaC) wavelets [14]. Basis functions of these wavelets can be numerically defined on triangular elements over irregular surfaces, which are supported either on triangular vertices (e.g. spherical and irregular wavelets) or faces (e.g. BLaC).

In the present study, we first compressed the cortical surface to create a multi-resolution model as spaces to define wavelets. Given the multi-resolution model, a face-based wavelet was then developed by designing scaling and wavelet basis functions at different resolution levels. The compressibility of cortical current densities using the face-based wavelet was tested on randomly located multiple sources and compared to a vertex-based wavelet, i.e. spherical wavelets [12]. Utilizing its compressibility, we further developed a novel SSI method by integrating the proposed face-based wavelet with L1-norm regularization to solve EEG/MEG inverse problem. Monte Carlo simulations were conducted to evaluate the performance of the proposed approach with comparison to a vertex-based wavelet method. Experimental data from an auditory induced language task was also adopted to evaluate the feasibility of the wavelet SSI.

## II. Methods

### A. Face-based Surface Wavelet

The proposed wavelets are defined on a multi-resolution model, which is obtained by hierarchically compressing the highly convoluted cortical mesh to create a series of nested spaces for multi-level analysis [15]. The compression procedure is done by merging multiple triangles on the fine level $n$ into one triangle on the coarse level $n+1$. An instant of

* This work was supported in part by NSF CAREER ECCS-0955260, OCAST HR09-125S, and DOT-FAA 10-G-008.

L. Ding is with the School of Electrical and Computer Engineering and Center for Biomedical Engineering, University of Oklahoma, Norman, OK 73019 USA (phone: 4053254577; fax: 4053257066; e-mail: leiding@ou.edu).

M. Zhu is with the School of Electrical and Computer Engineering, University of Oklahoma, Norman, OK 73072 USA (e-mail: Min.Zhu-1@ou.edu).

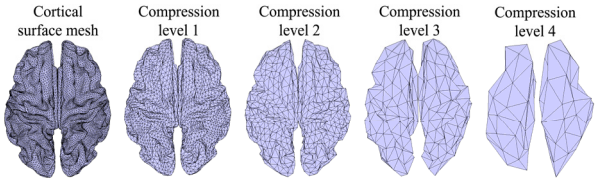


Figure 1. Illustration of original cortical surface mesh and its compressions at levels from one to four.

the cortical surface mesh and its multiple compression levels are shown in Fig. 1.

Each scaling function at the level $n$ is defined as one on a triangle and zeros otherwise, while scaling and wavelet functions at the coarse level $n+1$ are then computed from the linear combination of the scaling functions at level $n$ weighted by synthesis coefficients [14]. Similarly, scaling functions at level $n$ can be decomposed into the linear combinations of scaling and wavelet functions at coarse level $n$+1 weighted by analyses coefficients [14]. For convenience, let $A^n$, $B^n$ denote analysis matrices and $P^n$, $Q^n$ are synthesis matrices. Given analyses and synthesis matrices, functions defined on the original mesh can be iteratively compressed and reconstructed:

$$\text{Analysis:} \quad \bar{x}^{n+1} = A^n \bar{x}^n, \ \bar{y}^{n+1} = B^n \bar{x}^n \tag{1}$$

$$\text{Synthesis:} \quad \hat{x}^n = P^{n+1} x^{n+1} + Q^{n+1} y^{n+1} \tag{2}$$

where $\bar{x}^n, \bar{y}^n$ and $\bar{x}^{n+1}, \bar{y}^{n+1}$ are vectors of scaling and wavelet coefficients at the fine level $n$ and the coarse level $n+1$, and $\hat{x}^n$ denote the vector of estimated scaling coefficients from the synthesis procedure.

The wavelet transform matrix at level $n$ is straightforward to be derived by iteratively performing analysis procedures:

$$W^n = \begin{bmatrix} \left(G^n\right)^{1/2} A^{n-1} A^{n-2} \cdots A^0 \\ B^{n-1} A^{n-2} \cdots A^0 \\ \vdots \\ B^1 A^0 \\ B^0 \end{bmatrix} \tag{3}$$

where $G^n$ is a diagonal matrix with the $i$th element as the area of $i$th triangle at the compression level $n$, known as Gram-Schmidt matrix [14]. The superscript $0$ denotes the cortical surface at the finest resolution (i.e. the CCD model).

### B. Wavelet Based Sparse Source Imaging (WB-SSI)

The wavelet based SSI algorithm can be mathematically stated as the following optimization problem:

$$\min \left\| W^n \bar{x}^0 \right\|_1 \qquad subject \quad to \quad \left\| \bar{g} - H\bar{x}^0 \right\|_2 < \beta \tag{4}$$

where $W^n$ is the wavelet transform matrix in equation (3). The vector $\bar{g}$ denotes EEG/MEG measurements and the matrix $H$ is the so-called lead field, which can be calculated by solving the EEG/MEG forward problem [1] with given conductive profile model, e.g. boundary element (BE) model.

The optimization problem in equation (4) can be solved by the second-order cone programming (SOCP) [16], which is implemented in a Matlab package named SeDuMi [17]. The regularization parameter $\beta$ can be estimated by applying the discrepancy principle [18].

### C. Simulation Protocol

The CCD model of cortical surface was obtained by segmenting structural MRI data from an averaged subject in FreeSurfer's sample data set (http://surfer.nmr.mgh.harvard.edu) and multi-resolution model was then constructed with four compression levels as shown in Fig. 1.

Seed triangles on the CCD model were randomly selected and gradually added with neighboring triangles to grow into extended patches to simulate cortical sources with certain extents. Dipole moments within each simulated source patch were computed as the multiplication of triangular area and dipole moment density (i.e. 100pAm/mm$^2$). Simulations were conducted 200 times in order to cover most parts of the brain. To investigate compressibility of these cortical patch sources using the proposed face-based wavelet, sources synthesized from wavelet coefficients thresholded to reach 10% coefficient ratio (CR) (which is defined as the ratio between the number of non-zero coefficients after thresholding and the number of active elements in the original source domain) were evaluated by metrics of area under receiver operating characteristic (ROC) curve, i.e. AUC [20], and relative error (RE) [21]. Complexities of brain activities involving simultaneous activations were also considered in simulations with different numbers of cortical sources (i.e. 1, 2, 3, 5 and 10).

To evaluate the performance of WB-SSI, MEG measurements were simulated based on a 148-channel MEG system as generated by two simultaneous activations (i.e. two randomly located cortical patch sources as discussed above). A three-compartment BE model was built to model three major tissues (the scalp, skull, and brain) of different conductivity (0.33/Ω.m, 0.0165/Ω.m, and 0.33/Ω.m) [19] for the calculation of the forward problem [1]. MEG measurements were then contaminated by Gaussian white noise with signal to noise ratio (SNR) as 20dB. The performance of the L1-norm regularization using the face-based wavelet was compared to the L1-norm regularization using the vertex-based wavelet, i.e. Spherical wavelet, in recovering EEG/MEG sources at multiple compression levels (from one to three). Their performances were assessed using metrics of AUC from detection theory [20], spatial dispersion (SD) [21] and distance of localization error (DLE) [21].

### D. Experimental Protocol

To test the performance with empirical data, the L1-norm regularization method with the proposed face-based wavelet was tested with auditory MEG data. One epilepsy patient performed an auditory word recognition task with the same protocol from [22] during the pre-surgical evaluation in United Hospital, St. Paul, MN. MEG recordings were acquired from 148-channel Magnes WH2500 neuromagnetometer array (4-D Neuroimaging, San Diego, CA, USA). After applying the band-pass filter of 0.1-20Hz and baseline correction using pre-stimulus data, epochs were averaged to produce the event-related field (ERF). Sources were analyzed using both spherical wavelet and face-based wavelet in time window of 200-300ms post-stimulus, which was reported to be associated with early auditory and language process [23].

## III. Results

Fig. 2 shows the synthesis performance of the face-based wavelet method at different compression levels using different numbers of sources (i.e. 1, 2, 3, 5 and 10) with the same CR as 10%. As indicated in the AUC metric (Fig. 2(a)), the two-level, three-level, and four-level wavelet compressions have high synthesis accuracies about 0.95 after thresholding across all conditions with different numbers of sources. The one-level compression has the worst AUC values while they are still around 0.7 even in case of 10 simultaneously active and randomly located sources. The overall performance indicated

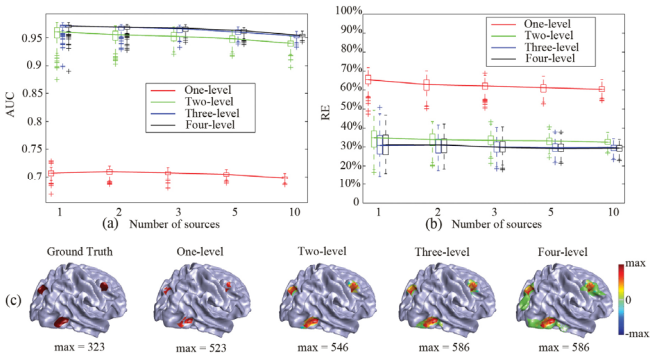


Figure 2. Performance of the face-based wavelet analysis at different compression levels with different number of sources (1, 2, 3, 5 and 10). (a) AUC. (b) RE. (c) An example of three sources and its synthesized results at levels one to four.

by the RE metric (Fig. 2(b)) shows that, for different numbers of sources, three-level and four-level compressions have the least RE values. Examples with three simulated cortical sources are provided in Fig. 2(c) for visual inspections of synthesized sources at different compression levels. The spatial extent of sources from the one-level compression is smaller than simulated ones, while sources from the three-level and four-level compressions are smoothed, which explains their high AUC values since the AUC metric favors smooth distributions.

Fig. 3 compares the performance of L1-norm regularization methods with the proposed face-based wavelet and the vertex-based Spherical wavelet in inverse source

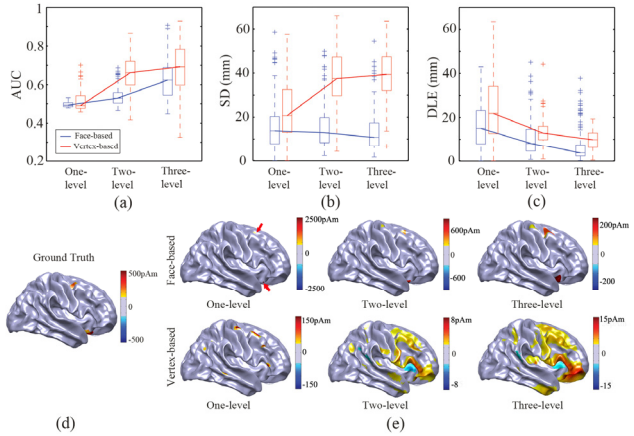


Figure 3. Performance of inverse source reconstruction with the face-based and vertex-based wavelets. (a) AUC. (b) SD. (c) DLE. (d) An example of two non-uniform sources. (e) Estimated sources in (d) using two methods at levels one to three.

reconstructions. Reconstructed cortical current densities are displayed with thresholding 20% of individual maxima. Although the face-based wavelet indicates worse AUC values than the vertex-based wavelet at the two-level and three-level compressions, it has significantly lower DLE values indicating fewer localization errors and significantly lower SD values indicating fewer errors in estimating source extents. The reason for the relative high AUC values from the vertex-based wavelet is that the AUC metric favors smooth distributions (as discussed in Fig. 2). It is evidenced from the given example in Fig. 3(e) that the L1-norm regularization with the vertex-based wavelet produce much smoothed results as compared with the L1-norm regularization using the face-based wavelet. Via visual inspection, it is suggested that the reconstructed sources from the vertex-based wavelet are actually worse than those from the face-based wavelet.

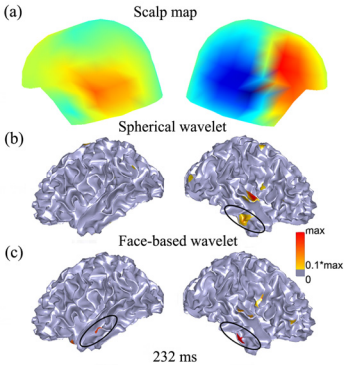


Figure 4. Comparison of the face-based and the vertex-based wavelet methods in estimating coritcal sources with auditory MEG data at 232 ms post-stimulus. (a) MEG scalp map. (b), (c) Sources from spherical and face-based wavelet at the analysis level of three.

Reconstructed cortical current sources underlying MEG data from the language task are shown in Fig. 4. Magnetic scalp maps at 232ms post-stimulus indicate that possible current sources origin from both hemispheres but more dominant on the right side. Cortical current sources are reconstructed from magnetic fields using spherical wavelet (vertex-based) and face-based wavelet via L1-norm regularizations. Display threshold of cortical sources is set as 10% of individual maxima. Dominant activities are observed in the right superior and medial temporal regions in both two methods, while the left medial temporal activations are only observed in the face-based wavelet method. The temporo-parietal activation and bilaterally medial temporal activations are supported by literatures [23] for the auditory induced early language processing around 200-300ms, which are believed to be associated with decoding of phonological and sematic components of words.

## IV. Discussion

In the present study, we proposed a novel wavelet method defined on triangular surfaces, which is able to compress brain activations on the highly folded cortical surface and can be further implemented in L1-norm regularization to solve EEG/MEG inverse problems. The present study indicated the compressibility of cortical sources using the proposed face-based wavelet, and the improved accuracy in recovering cortical sources using the L1-norm regularization with the face-based wavelet as compared with the vertex-based wavelet in simulations. Reconstructed sources from experimental data further demonstrated the improved performance of the L1-norm regularization with the use of the face-based wavelet in detecting brain activations.

The present results suggest that the proposed face-based wavelet is capable of providing a sparse representation of cortical current densities with a few numbers of coefficients without a significant decrease in accuracy. Although synthetic accuracy of the one-level wavelet analysis is relative low with AUC of around 0.7, the performance obviously improves when increasing the analysis level from one to two. However, the improvement from the two-level analysis to the four-level analysis is very limited. At the levels of three and four, syntheses from coefficients with 10% CR achieve the highest performance with AUC around 0.95 and RE around 30% (Fig. 2(a)). Comparing performances at the same analysis level, the flat trends of median values of both AUC and RE across different numbers of sources imply that the synthetic accuracy is not sensitive to the number of brain activations.

The proposed face-based wavelet analysis is then implemented into the L1-norm regularization framework to solve EEG/MEG inverse source reconstruction problems. Simulation results with two randomly located sources suggest that the inverse solver integrated with the proposed face-based wavelet has better performance than the inverse solver integrated with the vertex-based wavelet in terms of source localization accuracy (evaluated by SD and DLE) and source extent estimation accuracy (evaluated by SD) (Fig. 3 (a-c)). The relative higher AUC values from the vertex-based wavelet are due to smooth source distributions from its reconstructions, as visualized from examples given in Fig. 3 (e). When increasing the analysis level of wavelets analysis levels, all metrics (i.e. AUC, SD and DLE) indicate improved performance for the face-based wavelet method, while increased SD values in the vertex-based method imply more severe blurredness in inverse solutions.

In the analysis of experimental data from an auditory induced language task, the L1-norm regularization with the face-based wavelet further demonstrates its ability in reconstructing multiple simultaneous brain activations by successfully detecting bilateral symmetrical medial temporal activations, while the L1-norm regularization with vertex-based wavelet fails to detect the left medial temporal source. The L1-norm regularization with the proposed novel face-based wavelet will benefit researches in studying higher cognitive functions, e.g. language processing, which usually involves multiple brain regions [23].

In the present study, a feasible sparse representation of cortical current activities concerned as sources for EEG/MEG signals is achieved using the surface wavelet. Via integrating the surface wavelet with the L1-norm regularization [5, 6], a novel wavelet based sparse source imaging is developed. It is demonstrated that the WB-SSI technique can achieve improved reconstruction accuracy of source locations and extents in both simulations and experiments. The WB-SSI technique can become a promising non-invasive tool to inspect complex brain activations of significant importance in studying brain functions and networks.

## ACKNOWLEDGMENT

The authors thank Drs. Wenbo Zhang and Deanna Dickens from Minnesota Epilepsy Group, P.A. at United Hospital, St Paul, MN for generously sharing epilepsy data.

## REFERENCES

[1] S. Baillet, J. C. Mosher, and R.M. Leahy, "Electromagnetic brain mapping," *Signal Processing Magazine, IEEE,* vol. 18, pp. 14-30, 2001.

[2] A. M. Dale and M. I. Sereno, "Improved localizadon of cortical activity by combining EEG and MEG with MRI cortical surface reconstruction: A linear approach," *J. Cognitive Neuroscience,* vol. 5, pp. 162-176, 1993.

[3] R. Grech, T. Cassar, J. Muscat*, et al.*, "Review on solving the inverse problem in EEG source analysis," *Journal of NeuroEngineering and Rehabilitation,* vol. 5, 2008.

[4] K. Uutela, M. S. Hämäläinen, and E. Somersalo, "Visualization of magnetoencephalographic data using minimum current estimates," *NeuroImage,* vol. 3S, p. 168, 1999.

[5] L. Ding and B. He, "Sparse Source Imaging in Electroencephalography with Accurate Field Modeling," *Hum Brain Mapp* vol. 29, pp. 1053-1067, 2008.

[6] L. Ding, "Reconstructing cortical current density by exploring sparseness in the transform domain," *Phys in Med Biol,* vol. 54, pp. 2683-2697, 2009.

[7] S. Haufe, R. Tomioka, T. Dickhaus*, et al.*, "Large-scale EEG/MEG source localization with spatial flexibility," *Neuroimage,* vol. 54, pp. 851-859, 2011.

[8] F. Darvas, D. Pantazis, E. Kucukaltun-Yildirim, and R. M. Leahy, "Mapping human brain function with MEG and EEG: methods and validation," *NeuroImage,* vol. 23, Supplement 1, pp. S289-S299, 2004.

[9] F. Rosenow and H. Lüders, "Presurgical evaluation of epilepsy," *Brain,* vol. 124, pp. 1683-1700, 2001.

[10] E. Candes and J. Romberg, "Sparsity and Incoherence in Compressive Sampling," *Inverse Problems,* vol. 23, pp. 969-985, June 2007.

[11] S. Mallat, *A wavelet tour of signal processing: the sparse way*. Burlinton, MA: Academic Press, 2009.

[12] P. Schröder and W. Sweldens, "Spherical wavelets: Efficiently representing functions on the sphere," *Computer Graphics*, 1995.

[13] S. Valette and R. Prost, "Wavelet-based progressive compression scheme for triangle meshes: wavemesh," *Visualization and Computer Graphics, IEEE Transactions on,* vol. 10, pp. 123-129, 2004.

[14] G. P. Bonneau, S. Hahmann, and G. M. Nielson, "BLaC-wavelets: a multiresolution analysis with non-nested spaces," in *Visualization '96. Proceedings.*, 1996, pp. 43-48.

[15] M. Lounsbery, T. D. DeRose, and J. Warren, "Multiresolution analysis for surfaces of arbitrary topological type," *ACM Trans. Graph.,* vol. 16, pp. 34-73, 1997.

[16] M. S. Lobo, L. Vandenberghe, S. Boyd, and H. Lebret, "Applications of second-order cone programming," *Linear Algebra and its Applications,* vol. 284, pp. 193-228, 1998.

[17] J. F. Sturm, "Using SeDuMi 1.02, A Matlab toolbox for optimization over symmetric cones," *Optimization Methods and Software,* vol. 11, pp. 625-653, 1999/01/01 1999.

[18] A.V. Morozov, "On the solution of functional equations by the method of regularization," *Soviet. Math. Dokl*., vol. 7, pp. 414-417, 1966.

[19] Y. Lai, v. Drongelen, L. Ding*, et al.*, "Estimation of in vivo human brain-to-skull conductivity ratio from simultaneous extra- and intra-cranial electrical potential recordings," *Clin Neurophysiol* vol. 116, pp. 456-465, 2005.

[20] C. E. Metz, D. J. Goodenough, and K. Rossmann, "Evaluation of Receiver Operating Characteristic Curve Data in Terms of Information Theory, with Applications in Radiography," *Radiology,* vol. 109, pp. 297-303, November 1, 1973 1973.

[21] A. Molins, S. M. Stufflebeam, E. N. Brown, and M. S. Hämäläinen, "Quantification of the benefit from integrating MEG and EEG data in minimum ℓ2-norm estimation," *NeuroImage,* vol. 42, pp. 1069-1077, 2008.

[22] R. C. Doss, W. Zhang, G. L. Risse, and D. L. Dickens, "Lateralizing language with magnetic source imaging: Validation based on the Wada test," *Epilepsia,* vol. 50, pp. 2242-2248, Oct 2009.

[23] J. I. Breier, P. G. Simos, G. Zouridakis, and A. C. Papanicolaou, "Relative Timing of Neuronal Activity in Distinct Temporal Lobe Areas During a Recognition Memory Task for Words," *Journal of Clinical and Experimental Neuropsychology,* vol. 20, pp. 782-790, 1998/12/01 1998.